Supplementary Materials for

Harnessing theta-gamma coupled brainwaves using ultrasound for astrocyte revitalization and sustained neuropathic pain relief

Tien Thuy Phan[1#], Ho Jeong Kim[1,2], Keunhyung Lee[3], Dong-Wook Kang[4], Jung Moo Lee[1], Tai-Young Kim[1], Hyunjin Shin[4], Hye Eun Lee[5,6], Hyungju Park[7], Hyun-Woo Kim[4], Yee Joon Kim[1], Ji Young Mun[5], Jinhyoung Park[3,8], Kyu Pil Lee[9], C. Justin Lee[1,2], Joo Min Park[1,2*]
Correspondence to: joominp@ibs.re.kr

This PDF file includes:

Other Supplementary Materials for this manuscript include the following:

Methods

Animals

All experimental procedures were approved by the Institutional Animal Care and Use Committee (IACUC) at Institute of Basic Science (Approval number: IBS-2022-029). Mice were housed in groups of five, a 12:12 hour light/dark cycle (7 am-7 pm) was maintained. Behavioral testing was conducted between 9 am and 6 pm. Colonies of C57BL/6J (RRID: IMSR_JAX:000664), BDNF KIV knockout (generated as previously described [54]), TRPA1 knockout (KO; B6;129P-Trpa1tm1Kykw/J, RRID: IMSR_JAX:006401) mice were purchased from Jackson Laboratory and genotyped as previously described [29].

Partial sciatic nerve injury model (PCI)

The partial sciatic nerve injury model was conducted as previously described [28]. Briefly, adult male mice (8-10 weeks old) received a single unilateral crush injury to the sciatic nerve. Under isoflurane anesthesia, the right thigh was shaved, iodine treated and an incision was made along the thigh. The sciatic nerve, emerging from the sciatic foramen, was exposed and isolated from the muscle through blunt forceps dissection. An ultra-fine hemostat (Cat. No 13020-12, Fine Science Tools, Germany) was prepared with a custom spacer made of two layers of aluminum foil (15 µm thick) to create a 30 µm gap when fully closed. The sciatic nerve was carefully freed from the connective tissue, lifted by a fire-polished glass rod (Cat. No. 10061-12, Fine Science Tools, Germany), and placed between the aluminum foil gap on the hemostat (2-3 mm from the hemostat tip). The hemostat was then closed on the first locking position, held for 15s, and the nerve was carefully released. The wound was closed with sutures, and the mice were allowed to recover in Institute of Basic Science standard animal housing facility. All tools were autoclaved prior to the surgery, and strict aseptic technique was maintained throughout the procedure.

Ultrasound beam profile measurement

The output acoustic pressure of the H217 transducer (Sonic Concepts, Inc., USA) was measured using a needle hydrophone (NH1000, Precision Acoustics Ltd, UK) fixed with XYZ motorized stage. The ultrasound beam profile through the mouse spine was measured with a step size of 100 µm along the X and Y directions. The bean profile was visualized from 0.5 mm to 5.5 mm after the spine. The ultrasonic parameters such as frequency, input voltage and number of cycles in quantifying the beam profile were 500 kHz, 22 mVrms (0.77 W/cm^2) and 3 cycles respectively.

Ultrasound stimulation patterns

The ultrasound-based spinal cord stimulation (USCS) protocol involves bursts of 500 Hz (5 pulses) with a 40 Hz (25 ms) train pattern, totaling 800 pulses. The ultrasound pulses used in this protocol have a center frequency of 500 kHz and are characterized by continuous cycles over a 1 ms pulse duration. The continuous theta-burst ultrasound stimulation 200 Hz (cTBUS-200 Hz) consists of bursts of 200 Hz (4 pulses) with a 5 Hz (theta) train pattern. Similarly, the cTBUS-100 Hz includes a burst of 100 Hz (4 pulses) with 5 Hz (theta) train pattern. Both cTBUS-100 Hz and 200 Hz protocols also encompass a total of 800 pulses. The ultrasound pulses used in these

protocols have a center frequency of 500 kHz and are characterized by continuous cycles over a 3 ms pulse duration.

Von Frey Hair test

All sensory testing was performed between 9am-6pm in an isolated room maintained at 22 ± 2°C and 50 ± 10% humidity. For the mechanical threshold (Von-Frey filament) testing, mice were transferred from the standard keeping animal room to a transparent plastic cylinder (7 cm diameter and 20 cm height) placed on a mental mesh floor with 5x5 mm holes (mesh floor, Jeung Do Bio & plant co.). The mice were then habituated for at least one hour before the test. To access mechanical sensitivity, the withdrawal threshold of the injured hind paw was measured using a series of Von-Frey filaments (touch test sensory evaluation kit of 20, Cat. No 58011, Stoelting co.) (2.44, 2.83, 3,22, 3.61, 3.84, 4.08, 4.17, 4.31 nM, Exacta, North Coast Medical, USA; equivalent in grams to 0.04, 0.07, 0.16, 0.4, 0.6, 1, 1.4, 2). The 50% withdrawal threshold was determined using the 'up-down' method. The withdrawal response to the filaments regards as hind paw lift or flinch. The 0.4g filament was the first stimulus to be used, when there was no response then a higher diameter were applied, if there were response then the next lower diameter filament were applied. This process was repeated until no response was obtained.

Next generation sequencing

BCL files generated from the Illumina HiSeq2500 platform were converted to fastq format and demultiplexed according to index primer sequences. The data was then imported into Partek Genomics Suite (Flow ver. 10.0.21.0328; Copyright 2009, Partek, St. Louis, MO, USA) for further processing. Read quality for each sample was assessed using FastQC, and high-quality reads were aligned to the mouse genome assembly (mm10, Ensemble transcripts release 99). The aligned reads were normalized to the median ratio and quantified for analysis with DeSeq2. Differential analysis was performed using DeSeq2, and pathway analysis was conducted with reference to the KEGG database.

Catwalk gait analysis

The CatWalk XT version 10.6 (Noldus Information Technology, Netherlands) consists of a 1.3 m long black corridor on a glass plate with a green LED light inside, and placed in a dark and silent room (< 20 lx of illumination). Using the Illuminated Footprints technology, paws were captured by a high-speed video camera (100 frames per second) that was positioned underneath the glass. Mice walked freely across the runway into their home cage. The experiment was performed sheltered from noise in a darkened room with red light. The Catwalk XT 10.6 software package was used for data analysis. Prior to the experiment, each animal was trained over a two-day training period to become familiar with the task. A trial was regarded as successful if the animal did not show a maximum speed variation greater than 60%, did not exceed a walking speed of 400 mm/s and without stopping, turning around, or changing direction. Three compliant runs made up the testing run. For analysis, gait parameters were automatically generated after each footprint being manually checked and respectively labeled LF (Left Front), LH (Left Hind), RF (Right Front), and RH (Right Hind) paws. As the PCI-induced alterations develop in an

asymmetrical fashion, we analyzed parameters for the left and right side together and used RH/LH ratio for comparison.

Primary spinal astrocytes isolation, cell cultures and *in vitro* ultrasound stimulation

Primary cultured astrocytes were isolated from the spinal of C57BL/6J mouse pups at P0. Fine scissors were used to cut along the skin and the pup spine, spinal cord was collected with fine forceps and immediately put in cold Hank's Balanced Salt Solution (HBSS). Tissues were evenly homogenized by pipetting, following a brief centrifuge to withdraw the HBSS. Homogenized tissues were resuspended in cell culture media contained 25 glucose, 4 L-glutamine, 1 sodium pyruvate (in mM), 10% heat-inactivated horse serum (#26050-088, GIBCO), 10% heat-inactivated fetal bovine serum (#10082-147, GIBCO) and 10,000 units/ml penicillin–streptomycin (#15140-122, GIBCO) before spreading into cell culture dishes. Cultures were maintained at 37°C in a humidified 5% CO2 incubator. On 3 days in vitro (DIV), cells were vigorously washed with repeated pipetting and the media was replaced to get rid of debris and other floating cell types. During maintaining the culture before use, the media was replaced every 3-4 days. Cells were replated onto cover-glass coated with 0.1 mg/ml poly D-lysine (PDL, #P6407, Sigma-Aldrich) for experiments. In the *in vivo* experiments, we used the H217 transducer (0.5 MHz, focused single-element, effective diameter 33.0 mm x radius of curvature 63.2 mm) from Sonic Concepts, Inc., USA. The output intensity was set at 0.77 W/cm^2. In contrast, for the *in vitro* cell culture experiments, we used the Olympus V301-SU transducer (0.5 MHz, single-element, effective diameter 25 mm) due to experimental constraints. Based on the low-intensity (<3 W/cm^2) threshold observed for the analgesic effect in the *in vivo* study, we applied cTBUS-200 Hz stimulation using the Olympus transducer in the *in vitro* experiments. For this purpose, we selected a minimum stimulation value of 500 mVrms and a maximum stimulation value of 990 mVrms, corresponding to output intensities of 2.4 W/cm^2 and 2.8 W/cm^2, respectively. Notably, both of these stimulation intensities are lower than the 3 W/cm^2 intensity observed in the *in vivo* experiments.

Immunocytochemistry

Cells were fixed with 4% paraformaldehyde (PFA) at room temperature (RT) for 10 minutes and subsequently permeabilized by 0.03% Triton X-100 PBS with 2% donkey serum and 2% goat serum. After incubation in blocking solution for 1 hour at RT, cells were incubated overnight at 4 °C with primary antibodies: GFAP (1:1000, Millipore AB5541), GABA (1:1000, Sigma-Aldrich AB175), BDNF (1:1000, abcam ab108319). Cells were washed with PBS 3 times before staining with secondary antibodies (Goat Anti-Chicken Alexa Fluor® 488, Goat Anti-Rabbit Alexa Fluor®647, Donkey Anti-Genuine Pig Alexa Fluor® 594). Cells were washed with PBST 3 times with the DAPI incubation in the last wash (1:1000, Thermo scientific 66248). Cover-glass was mounted with nail polish into glass-slide and store in 4°C overnight.

Immunohistochemistry

Mice were perfused with phosphate-buffered saline (PBS) followed by 4% paraformaldehyde (PFA) through a peristaltic pump. Spinal cord tissue was immediately collected and incubated in 4% PFA overnight. The tissue was then sectioned at 30 μM into cold PBS using vibratome Leica

VT1000S and store at 4°C. For spinal cord immunohistochemistry, spinal sections were immunolabeled for GFAP, GABA, BDNF, Iba1 (1:1000, ab225260), PV (1:1000, Swan 235). Briefly, tissue was washed with PBS/0.3% Triton X-100 (PBST) for 4 times, blocked with PBST containing 5% normal goat serum for 2 hours at RT, and then incubated overnight with primary antibodies at 4°C. The next day, tissue was washed with PBST for 4 times followed by 2 hour of secondaries (Goat anti-Rabbit Alexa Fluor® 488, Goat anti-Mouse Alexa Fluor® 647, Goat Anti-Chicken Alexa Fluor® 647, 1:800; abcam) at RT. Tissue was then washed with PBST for 4 times before mounted onto glass slides and cover with DAPI-containing mounting medium VECTASHIELD® (Vector laboratories). Imaging for quantification of GFAP, Iba1, GABA and BDNF expression were conduct at 40X on Nikon Ti-e Eclipse with PFS microscopy and whole spinal cord section at 20X on Axio Scan Z1.

Immunoblotting

Proteins were isolated and pooled from spinal cord, homogenized with pestle after freeze and thaw in Tissue Lysis/Extraction Reagent (Sigma-Aldrich). Next, SDS–PAGE and western blotting were performed Thirty micrograms of proteins were loaded for each lane on a 4–12% Tris-glycine gel (Invitrogen), resolved and transferred onto polyvinylidene difluoride membrane. On blocking 1 hour at RT with 5% milk powder (AppliChem, Darmstadt, Germany) diluted in double distillate water, the blotted proteins were incubated overnight at 4°C with goat polyclonal anti-BDNF antibody diluted 1:1000 (Abcam, ab60210), KCC2 at 1:1000 (Santa Cruz Biotechnology) and mouse monoclonal anti-GAPDH or β-Actin antibody diluted 1:10000 (Abcam, Cambridge, UK). Next, the membrane was incubated for 2 hours at RT with the secondary antibodies ECL peroxidase-labelled anti-goat or mouse antibody (1:2000; Amersham Biosciences, Freiburg, Germany). Labelled proteins were detected by chemiluminescence using the ECL Prime Western Blotting Detection Reagents (Amersham Biosciences) on Image lab software. Band intensities were analyzed using the open-source software ImageJ and calculated as expression relative to the housekeeping gene (GAPDH or β-Actin). Every lane was analyzed with the plot analysis tool of ImageJ and the area of the peak corresponding to the band was used as intensity value.

RNA isolation and RT-PCR

Total RNA was isolated from the tissue samples using the RNeasy Mini Kit (Qiagen, Valencia, CA, USA) according to the manufacturer's instructions. RNA concentration and purity were assessed using a NanoDrop ND-1000 Spectrophotometer (Thermo Fisher Scientific, Waltham, MA, USA). cDNA synthesis was performed using the High-Capacity cDNA Reverse Transcription Kit (Applied Biosystems, Foster City, CA, USA) with 1 μg of total RNA per reaction. PCR amplification was performed using specific primers for BDNF and GAPDH as an internal control. The sequences of the primers were as follows: BDNF exon 1 forward, 5'- GTG TGA CCT GAG CAG TGG GCA AAG GA-3', BDNF exon 2 forward, 5'- GGA AGT GGA AGA AAC CGT CTA GAG CA -3', BDNF exon 3 forward, 5'- GCT TTC TAT CAT CCC TCC CCG AGA GT -3', BDNF exon 4 forward, 5'- CTC TGC CTA GAT CAA ATG GAG CTT C -3', BDNF exon 5 forward, 5'- CTC TGT GTA GTT TCA TTG TGT GTT C-3', BDNF exon 6 forward, 5'- GCT GGC TGT CGC ACG GTT CCC ATT-3', BDNF exon 7 forward, 5'- CCT GAA AGG GTC

TGC GGA ACT CCA-3', BDNF exon 8 forward, 5'- GTG TGT GTC TCT GCG CCT CAG TGG A-3', BDNF exon 9 forward, 5'- CCC AAA GCT GCT AAA GCG GGA GGA AG-3'. BDNF reverse, 5'- GAA GTG TAC AAG TCC GCG TCC TTA-3', GAPDH forward, 5'-GGCTGTATTCCCCTCCATCG-3', GAPDH reverse, 5'-CCAGTTGGTAACAATGCCATGT-3'. PCR products were visualized on 2% agarose gels stained with ethidium bromide. The relative expression of BDNF mRNA was calculated using the $2^{-\Delta\Delta Ct}$ method. Data were expressed as mean ± SEM of three independent experiments.

FACs analysis

BDNF-GFP plasmid was transfected to HEK-293T cell using Expi293™ expression system (ThermoFisher, Cat. A14635). BDNF-GFP tag cell media was harvest and transfer to primary astrocyte culture prior to the LI-cTBUS stimulation 5 minutes. After LI-cTBUS stimuatlion, primary astrocytes were harvested by 0.25% Trypsin and mixed with cold PBS for FACs sorting (FACsCanto II). Cells were purified with single-cell exclusive gating.

Intrathecal injection

The mice were anaesthetized under 3% of isoflurane for induction and 1–2% for maintenance. Intrathecal injection was performed using a winged infusion set connected to a 50-ml Hamilton syringe. BDNF (50 ng/kg) was injected into the intervertebral space in the lumbar region between L5 and L6 level of the spinal cord. A reflexive flick of the tail was considered as a sign of the accuracy of each injection. Behavioral testing was assessed by Von-Frey test as described earlier.

Fiber photometry in spinal cord

Thy1_GCamp6f mice were fixed using stereotaxic (using multi-functional adaptors #68091, RWD) and anesthetized with 2% isoflurane for laminectomy. Briefly, an incision was made over the back, and surrounding tissues and spinal bones were carefully dissected to expose the spinal cord. The mice were positioned on a 38°C heat pad with a soft cushion for stability. For recording, an optical cannula was positioned on the spinal cord. The ultrasound transducer was positioned below the target area, and the anesthesia level was reduced from 2% to 0.5%. Calcium signals were confirmed prior to the application of cTBUS (200 Hz) stimulation. Light emitting diodes at 488 nm (GCaMP stimulation wavelength) and 405 nm (control for artifactual fluorescence) (Doric) were coupled to a 400 μm 0.4 N.A0.22 optical fiber (ZF1.25, Doric). The emitted light was collected by the same optical fiber, passed through a GFP filter and focused onto a fluorescence detector (fluorescence mini cube, Doric) where the two output signals were separated based on modulation frequency. Samples were collected at a frequency of 330 Hz. Recordings were made in the lumbar sacral region during both ultrasound stimulation (40s) and no stimulation (40s).
Data were extracted and analyzed using custom-written scripts. To normalize the data, the control channel was fitted to and then subtracted from the raw trace, resulting in the calculation of ΔF/F.

Electron microscopy analysis

Ultrastructural analysis was performed using transmission electron microscopy (TEM). Astrocytes in each group were grown on coverslips. The samples were immediately fixed with 1 % glutaraldehyde–1 % paraformaldehyde solution for 1 h and postfixed in 1 % osmium tetroxide for 1 h at 4°C. The block was stained with 1 % uranyl acetate and dehydrated with a graded ethanol

series. The samples were embedded in epoxy medium (EMS, Hatfield, PA) and sectioned into 60-nm sections using an ultramicrotome (Leica Microsystems, Wetzlar, Germany). Then, the sections were double-stained with UranyLess for 2 min and 3% lead citrate for 1 min. The stained sections were viewed on a Tecnai 20 TEM (Thermo Fisher Scientific, Waltham, MA, USA) at 120 kV, and images were captured using a US1000X–P camera 200. The acquired images were stitched together using Photomontage software (Thermo Fisher Scientific, Waltham, MA, USA). The area of ER and number of lysosomes was analyzed using Image J.

Kainic acid injection

Kainic acid (20 mg/kg) was intraperitoneally injected to induce BDNF elevation in wild-type mice as previously described [54]. Mice were euthanized 6 hours after the injection, mPFC and spinal lumbar sacral samples were collected for Western blot experiments to validate the BDNF antibody (Supplementary Fig. 9).

Apoptosis assay

Mice were perfused for spinal cord extraction. Apoptosis cell assay was conduct using the TUNEL assay kit-HPR-DAB (ab206386). Briefly, the spinal cord tissues were fixed with 4% PFA and sliced into 10 μm sections. The tissues were then fixed and hydrated with 4% PFA, followed by permeabilization with Proteinase for 10 minutes. The tissues were then washed with 1X TBS and immersed in 30% H_2O_2 diluted in methanol for activating endogenous peroxidases. Tissues were then washed and covered with TdT equilibrium buffer, followed by labeling with the Labeling reaction mix and incubated at 37°C for 90 minutes. Tissues were immersed with Stop buffer and blocked for 10 minutes at RT. Finally, tissues were developed using DAB solution for 15 minutes. Methyl Green counterstain solution was used for counterstaining, followed by washing with100% ethanol and xylene. The mounted samples were visualized at 20X on Axio Scan Z1.

Statistical information

Statistical analysis was performed using the GraphPad prism suite (GraphPad Software Inc., San Diego, CA). The sample size was determined based on significance testing, considering available number of neurons per in vitro experiment or mice from same litters. All means are presented as mean±s.e.m.

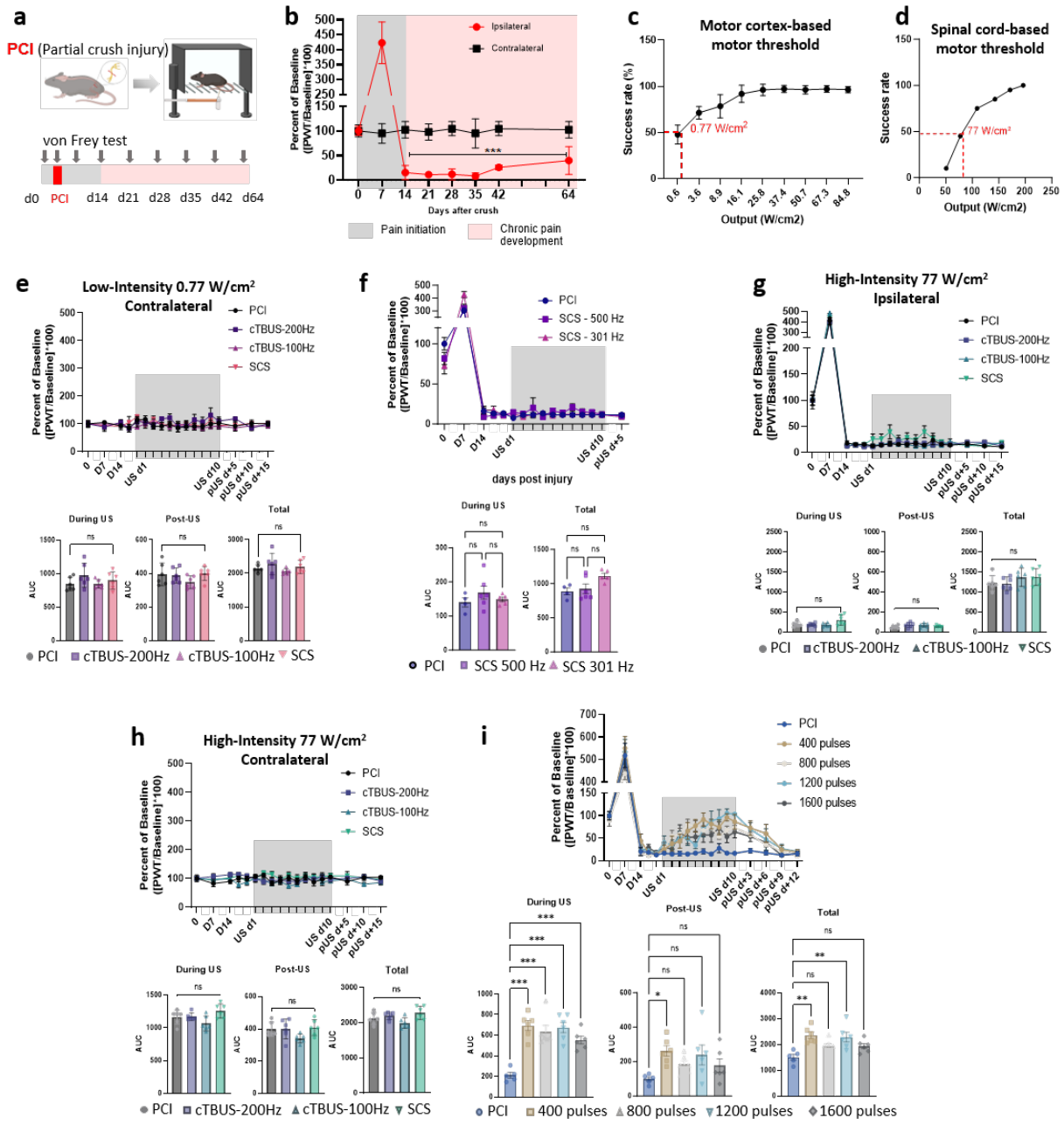

Figure. S1. LI-cTBUS induces analgesic effect rather than high-intensity.

(a) (Left) Partial crush injury (PCI) model (right) with pain threshold measurement schedule, arrow representing von-Frey test. **(b)** Percentage of withdrawal threshold (WT) in PCI model. ***p<0.001, two-way ANOVA with Tukey's multiple comparison test, N=12. **(c)** Minimum intensity of cortical ultrasound stimuli to elicit motor response (MEP): 50% threshold of ultrasound evoked motor response at 22 mVrms (0.77 W/cm^2). **(d)** Minimum intensity of spinal ultrasound stimuli to elicit motor response (MEP): 50% threshold of ultrasound evoked motor response at 250 mVrms (77 W/cm^2). **(e)** Percentage of withdrawal threshold (WT) in the contralateral side under

low intensity (0.77 W/cm^2) ultrasound stimulation, N=6. **(f)** Percentage of WT in SCS at 301 Hz with a 3 ms pulse duration and 500 Hz with a 25 ms pulse duration, N=6. **(g)** Percentage of WT in the ipsilateral side among PCI model groups treated with SCS, cTBUS-100 Hz and cTBUS-200 HZ with high intensity (top), area under curve of WT during and post ultrasound treatments (bottom), N=6. (**h)** Percentage of WT in the contralateral side under high intensity (77 W/cm^2) ultrasound stimulation, N=6. **(i)** Percentage of WT under time-dependent ultrasound stimuli patterns, N=6. ***$p<0.001$, two-way ANOVA with Tukey's multiple comparison test. ns: non-significant, $p>0.99$.

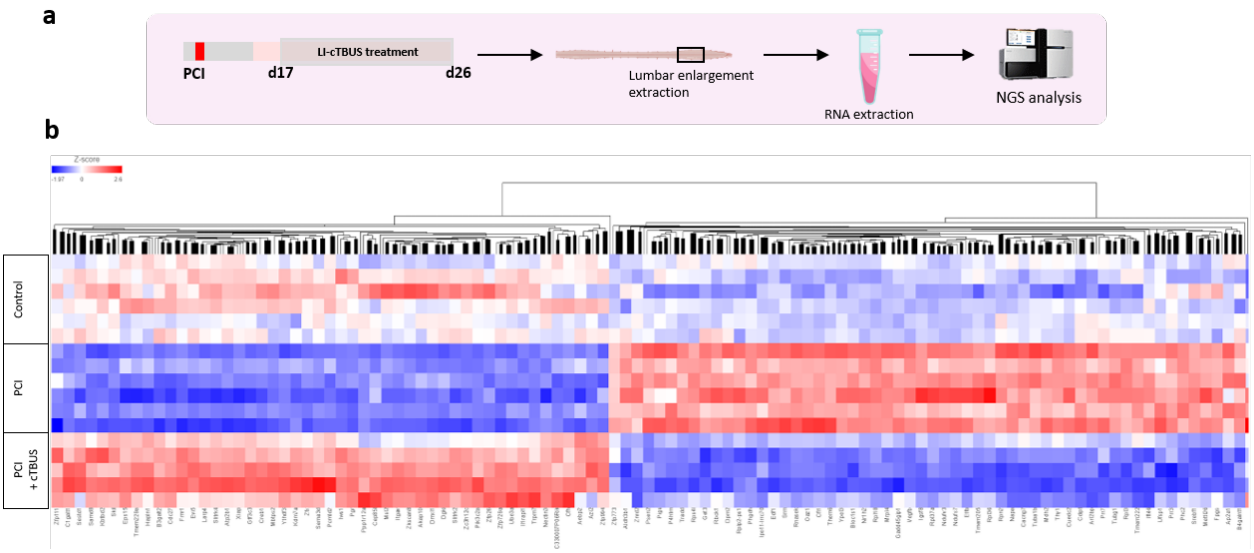

Figure. S2. Whole genome sequencing uncovers characteristics of cTBUS effects on PCI model.

(a) Schematic diagram of RNA-seq process. **(b)** Bulk RNA sequencing results revealed 14949 genes expression among three groups, N=6/group.

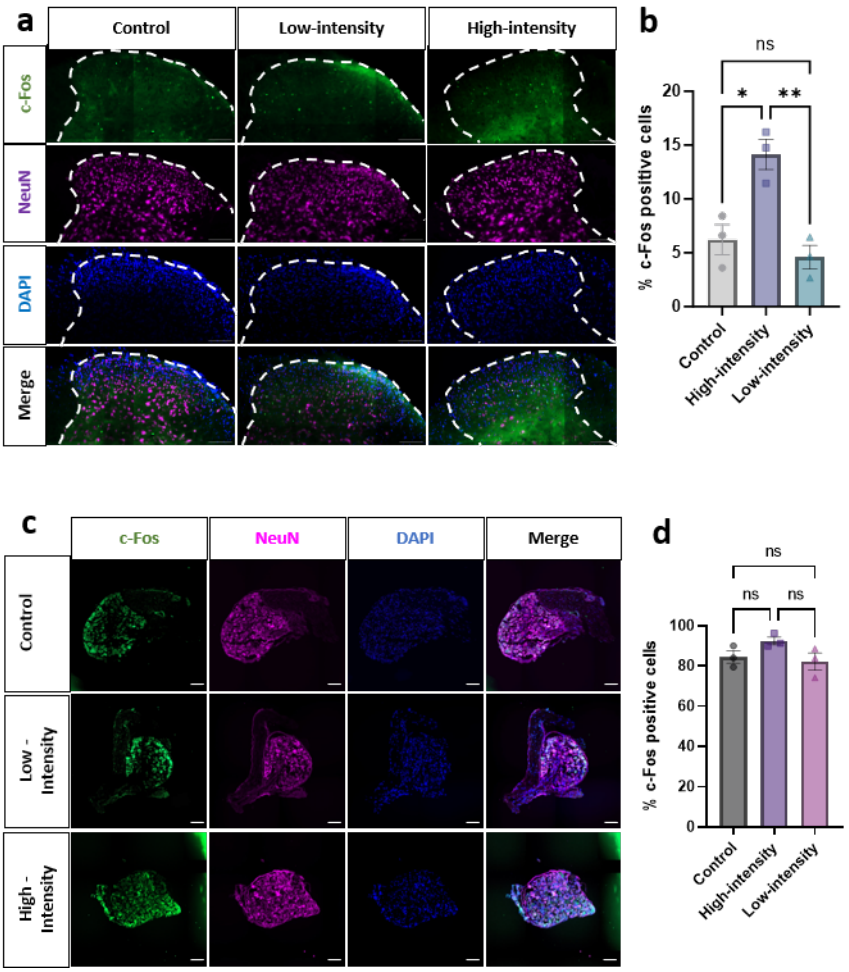

Figure. S3. Absence of neuronal activation in dorsal horn and dorsal root ganglia of normal mice with LI-cTBUS Stimulation.
(a) Immunohistochemistry representative image of c-Fos and NeuN expression level in wild-type mice spinal cord under high-intensity (77 W/cm^2) and low-intensity ultrasound (0.77 W/cm^2). Scale bar: 100 µm. **(b)** Quantification of c-Fos positive NeuN in percentage. *p<0.01, **p<0.005, one-way ANOVA with Tukey's multiple comparison test. ns: not significant. **(c)** Immunohistochemistry representative image of c-Fos and NeuN expression level in wild-type mice dorsal root-ganglia under high-intensity (77 W/cm^2) and low-intensity ultrasound (0.77 W/cm^2). Scale bar: 100 µm. **(d)** Quantification of c-Fos positive NeuN in percentage using one-way ANOVA with Tukey's multiple comparison test. ns: non-significant.

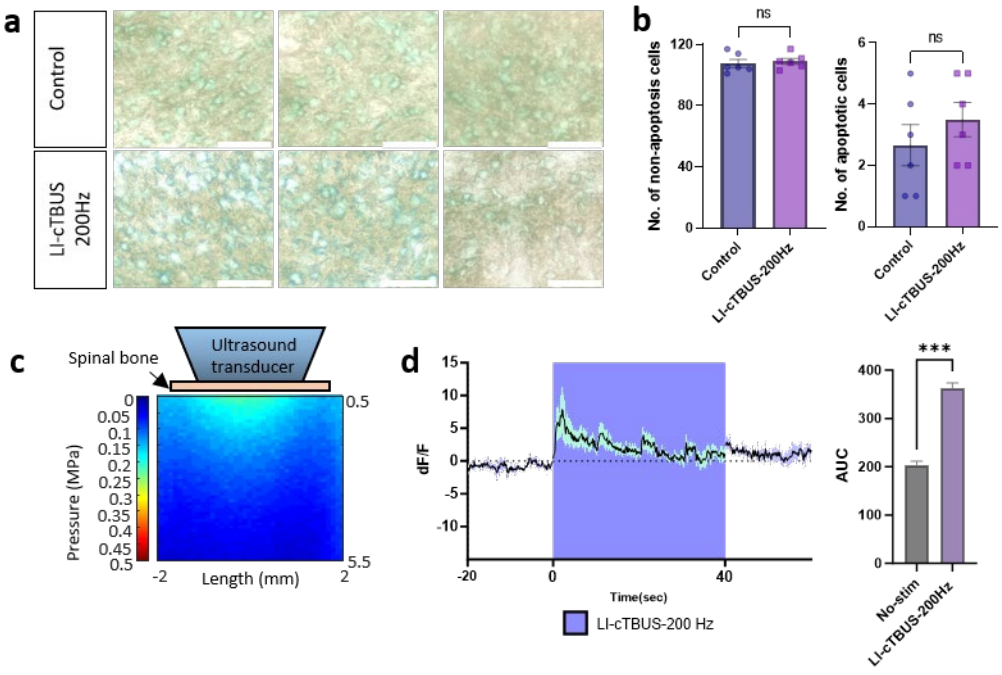

Figure. S4. Safety profile and physical properties of LI-cTBUS stimulation over the spinal cord. **(a)** Representative HRP-DAB TUNEL assay showing detection of apoptotic cells under ultrasound effect. Apoptotic cells are depicted in brown, while live cells are shown in blue. **(b)** Quantification of apoptotic (p=0.362) and non-apoptotic cells (p=0.688) using a two-sample t-test. ns: non-significant, N=6. **(c)** Ultrasound beam profile through the mouse spine with ultrasound frequency at 500 kHz, input voltage at 0.77 W/cm^2 and 3 cycles. **(d)** (left) cTBUS-200 Hz stimulation at the spinal cord evoked Ca^{2+} response. (right) Area under curve of Ca^{2+} response in no-stim and cTBUS-200 Hz stimulation group. ***$p < 0.001$, two-sample t-test.

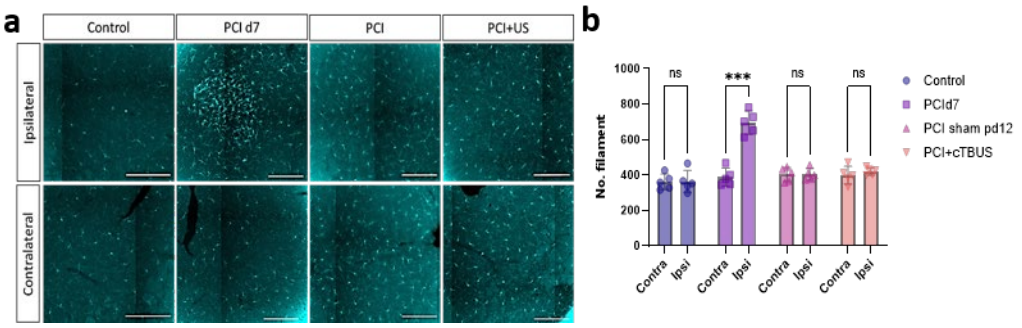

Figure. S5. Lack of effect of LI-cTBUS on microgliosis.

(a) Immunohistochemistry representative images of Iba1 (scale bar: 200 µm) during the pain progression in the PCI model. **(b)** Number of filaments in ipsilateral and contralateral side among the 4 groups. ***p<0.01, two-way ANOVA with Tukey's multiple comparison test. ns: non-significant, p>0.99.

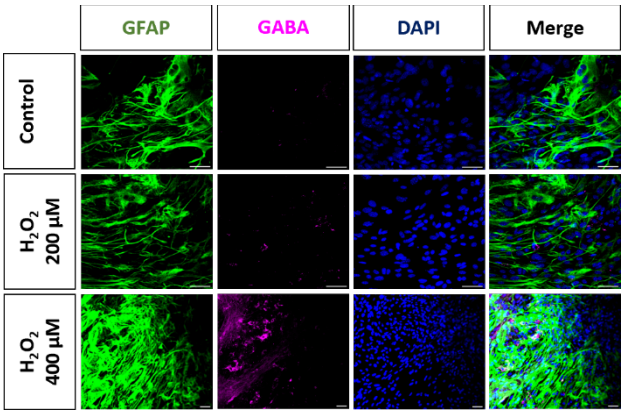

Figure. S6. Oxidative stress-induced astrogliosis.
H_2O_2-induced astrocyte stress and increased astrocytic GABA in a dose-dependent manner. Immunocytochemistry representative images of GFAP and GABA expression levels under H_2O_2 treatment.

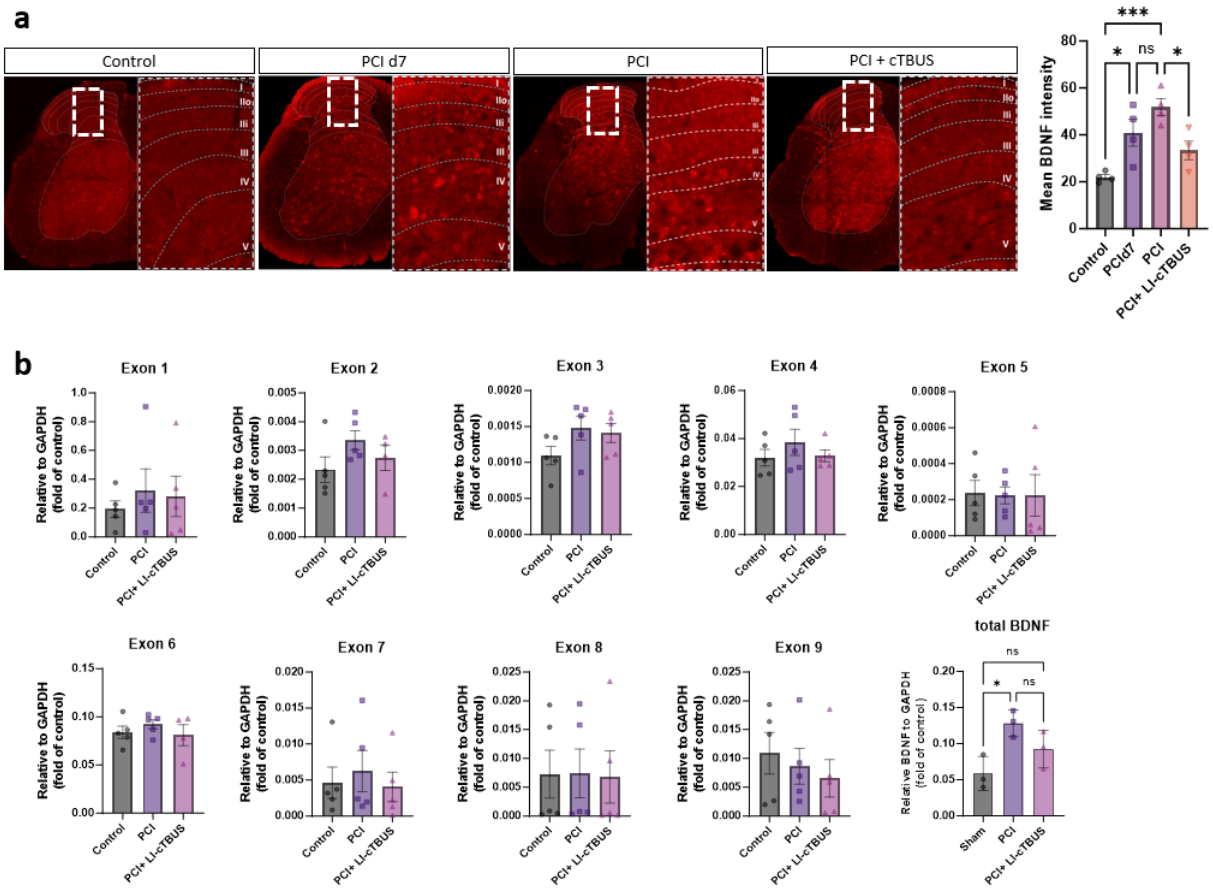

Figure. S7. LI-cTBUS induces analgesia involved in spinal BDNF protein signaling pathway. **(a)** (Left) BDNF expression level in spinal dorsal horn among four groups: control, PCI day 7, PCI and PCI+LI-cTBUS. (Right) Mean intensity of BDNF expression in dorsal spinal horn. **(b)** mRNA expression level of spinal BDNF. *p<0.01 ***p<0.001, one-way ANOVA with Tukey's multiple comparison test. ns: non-significant.

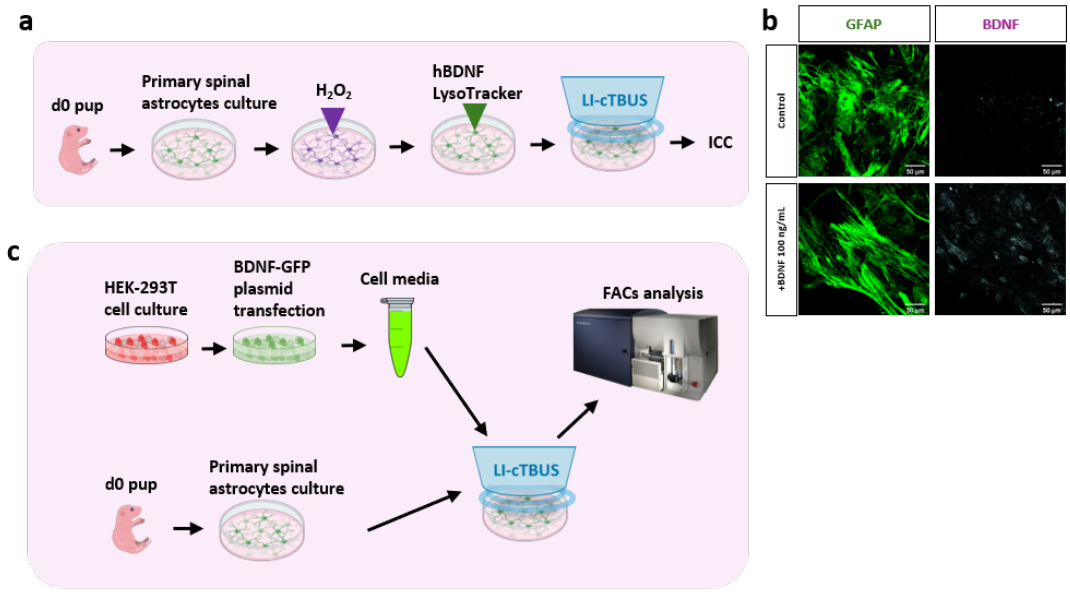
a
d0 pup
Primary spinal astrocytes culture
H_2O_2
hBDNF LysoTracker
LI-cTBUS
ICC
b
GFAP
BDNF
Control
+BDNF 100 ng/mL
c
HEK-293T cell culture
BDNF-GFP plasmid transfection
Cell media
FACs analysis
d0 pup
Primary spinal astrocytes culture
LI-cTBUS
d
20240306-Tube_003
SSC-A
FSC-A
P1
Tube: Tube_003
Population #Events %Parent %Total
All Events 10,000 #### 100.0
P1 4,168 41.7 41.7
P3 4,001 96.0 40.0
P5 3,420 85.5 34.2
P7 521 13.0 5.2
P2 1,905 19.0 19.0
P4 1,794 94.2 17.9
P6 1,771 98.7 17.7
P8 23 1.3 0.2
20240306-Tube_003
SSC-H
SSC-A
P3
20240306-Tube_003
FSC-A
FITC-A
P5
P7
20240306-Tube_003
SSC-H
SSC-A
P4
20240306-Tube_003
FSC-A
FITC-A
P6
P8

Figure. S8. LI-cTBUS facilitates BDNF uptake by spinal astrocytes.
(a) *in vitro* schematic experiment of LI-cTBUS 200 Hz stimulating spinal astrocytes. **(b)** hBDNF 100ng/mL was added in primary astrocyte culture after 24 hours of H2O2 treatment to increase basal BDNF levels. **(c)** Schematic illustration of FACs analysis for determine BDNF uptake in spinal astrocytes under LI-cTBUS stimulation. **(d)** FACs gaiting standard: P1-P8: death cells, fail positives; P7: GFP-positive cells.

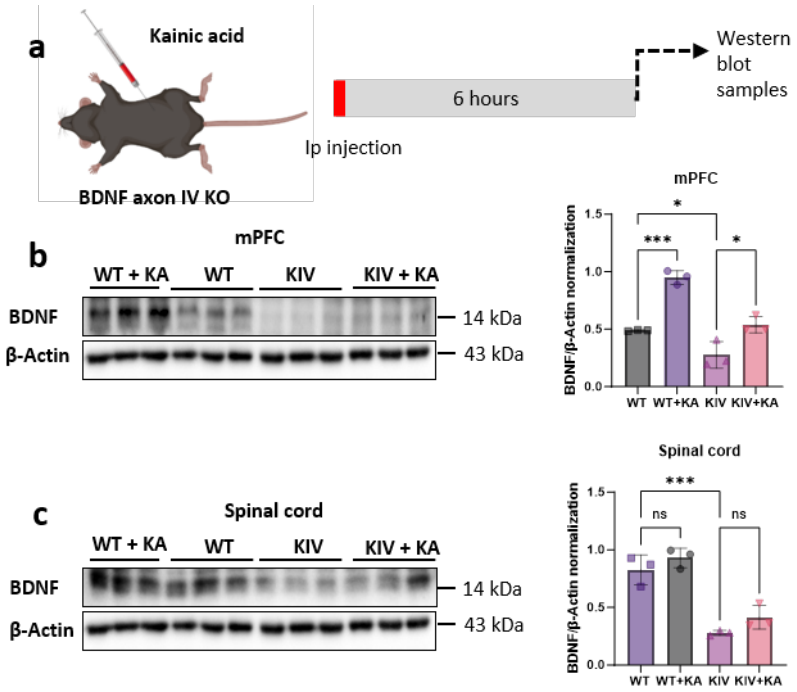

Figure. S9. Validation of BDNF antibody in neuronal BDNF axon IV knockout mice.

(a) Experimental paradigm for validating BDNF antibody. Kainic acid (KA) was intraperitoneally injected at a dose of 20 mg/kg into both wild-type mice and BDNF exon IV knockout mice (KIV) to elevate the brain BDNF level. Brain and spinal cord samples were extracted 6 hours after the injection. **(b)** BDNF protein expression level in mPFC among WT and KIV group with and without KA injection: KA significantly increases BDNF levels in the WT mPFC, ***p<0.01, one-way ANOVA with Tukey's multiple comparison test. However, BDNF exon IV knockout mice showed low levels of BDNF even after KA injection. *p=0.01, one-way ANOVA with Tukey's multiple comparison test. **(c)** BDNF protein expression level in spinal cord among WT and KIV group with and without KA injection. KA injection failed to elevate spinal BDNF level in KIV mice. ***p<0.01, one-way ANOVA with Tukey's multiple comparison test. ns: non-significant, p>0.99.

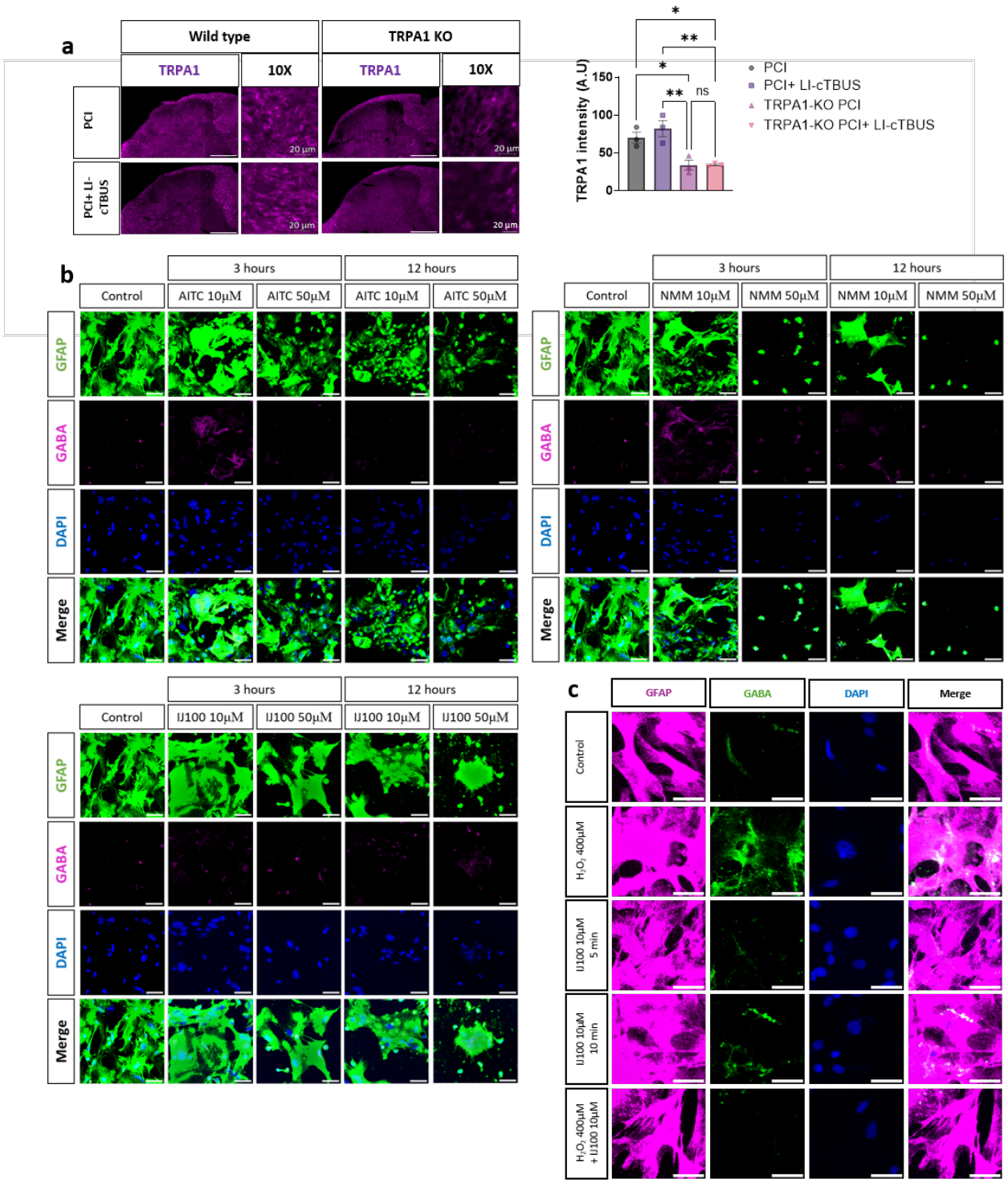

Figure. S10. TRPA1 involved in LI-cTBUS-induced analgesia.

(a) Immunohistochemistry of TRPA1 expression level in spinal dorsal horn of PCI WT and PI TRPA1 KO with and without cTBUS stimulation. TRPA1 expression intensity in spinal dorsal

horn (A.U). **p<0.01, one-way ANOVA with Tukey's multiple comparison test. ns: non-significant, p>0.99. **(b)** Immunocytochemistry representative images of primary astrocyte culture under prolonged treatment of TRPA1 agonists (AITC, NMM and IJ100) in dose and time-dependence, scale bar: 10µm. **(c)** Immunocytochemistry representative data of short-term TRPA1 agonist treatment in primary astrocyte culture, scale bar: 10µm.

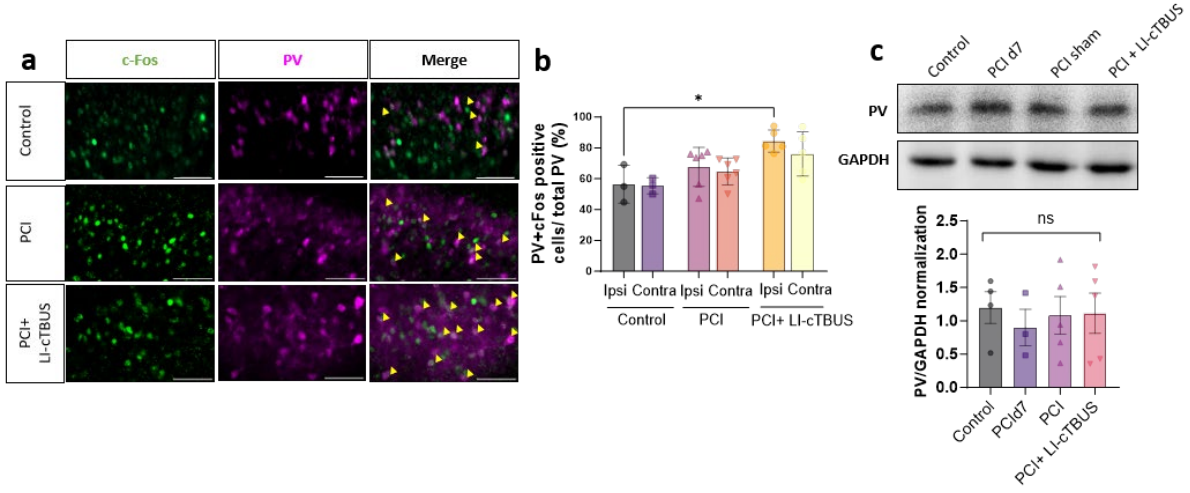

Figure. S11. Activation of spinal dorsal horn interneuron parvalbumin by cTBUS stimulation.

(a) Immunohistochemistry for PV expression and PV co-expressing c-Fos in spinal cord lumbar section L4-L5 among US-treated and non-US-treated PCI groups. **(b)** Quantification of PV/+c-Fos shows higher activated PV cells after US stimulation. **(c)** PV protein quantification does not show differences in total protein level. ***p<0.001, One-way ANOVA with Tukey's multiple comparison test. ns: non-significant, p>0.99.

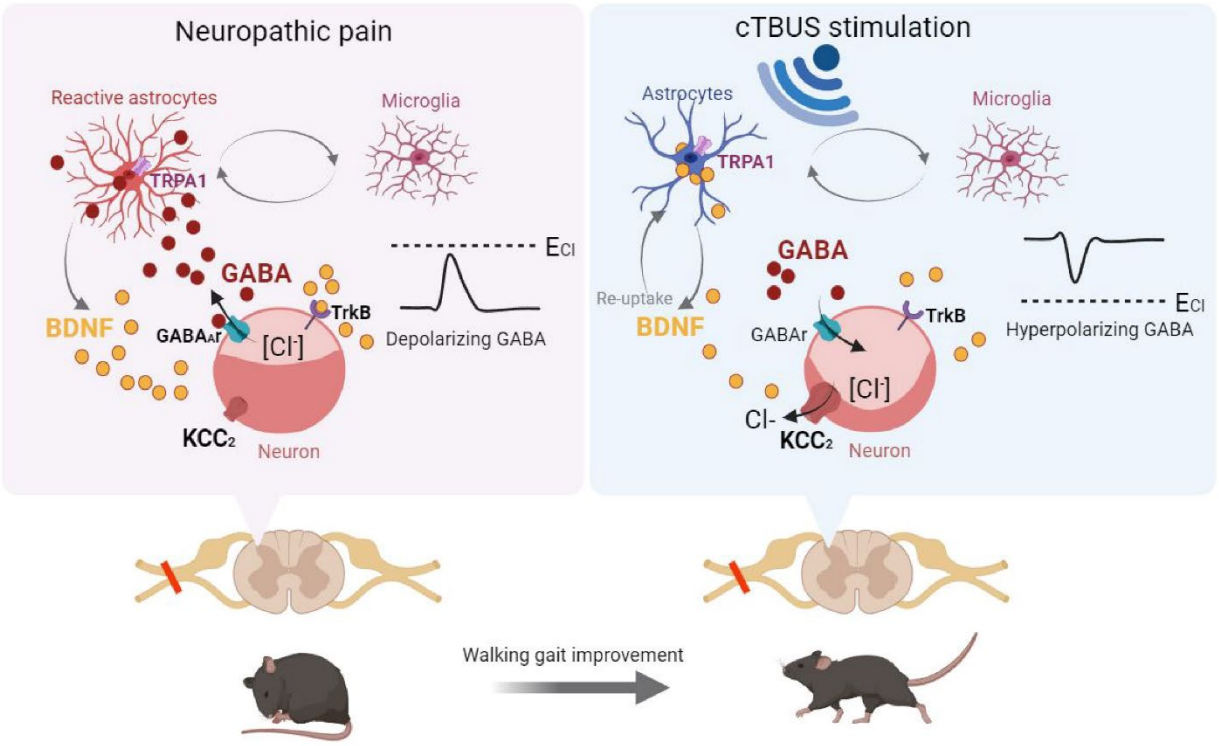

Figure. S12.

Low-intensity continuous theta-gamma ultrasound (LI-cTBUS) relieves neuropathic pain with lasting effects. These effects involved the enhancement of spinal BDNF uptake, balancing BDNF/TrkB/KCC2 to relieve pain. Furthermore, LI-cTBUS activates TRPA1, consequently reducing astrogliosis and aiding ultrasound-induced analgesia. LI-cTBUS normalizes transcriptomic response by modulating inflammation, BDNF/TrkB, and GABA pathway. Overall, low-intensity theta-burst ultrasound stimulation shows promise for alleviating neuropathic pain and opens up new possibilities for pain management.

Table S1.

Ultrasound H217 transducer intensity calibration for in vivo stimulation.

Sonic Concept H217 - Amplifier research				Average output (mVpp)	Negative Pressure (Mpa)	Corrected Pressure (Mpa)	Intensity (100%) (W/cm^2)	Mechanical Index
mVRMS	Trial 1 (mVpp)	Trial 2 (mVpp)	Trial 3 (mVpp)					
10	5.0	4.5	4.8	4.8	0.085	0.075	0.177	0.11
20	9.2	8.7	9.3	9.1	0.162	0.143	0.641	0.20
30	13.5	12.5	13.8	13.3	0.237	0.209	1.371	0.30
40	17.7	16.1	17.8	17.2	0.307	0.271	2.305	0.38
50	22.1	20.3	22.2	21.5	0.385	0.340	3.613	0.48
60	26.5	24.3	26.7	25.8	0.461	0.408	5.200	0.58
70	30.8	27.9	30.7	29.8	0.532	0.470	6.920	0.67
80	34.8	31.4	35.4	33.9	0.605	0.535	8.937	0.76
90	37.8	35.8	39.8	37.8	0.675	0.597	11.134	0.84
100	41.2	39.2	43.8	41.4	0.739	0.653	13.355	0.92
110	45.8	42.6	48.2	45.5	0.813	0.719	16.155	1.02
120	49.4	46.2	53.7	49.8	0.889	0.785	19.299	1.11
130	53.1	49.4	57.1	53.2	0.950	0.840	22.053	1.19
140	58.3	53.5	61.1	57.6	1.029	0.910	25.882	1.29
150	61.9	57.1	65.1	61.4	1.096	0.969	29.344	1.37
160	65.9	61.1	69.1	65.4	1.167	1.032	33.294	1.46
170	70.0	64.0	74.0	69.3	1.238	1.094	37.457	1.55
180	73.2	67.9	78.0	73.0	1.304	1.153	41.562	1.63
190	76.9	71.2	82.4	76.8	1.372	1.213	46.000	1.72
200	80.8	75.2	86.0	80.7	1.440	1.273	50.704	1.80
210	84.0	79.0	90.5	84.5	1.509	1.334	55.637	1.89
220	88.0	84.0	94.7	88.9	1.588	1.403	61.583	1.98
230	92.0	86.0	101.0	93.0	1.661	1.468	67.394	2.08
240	96.0	89.0	105.0	96.7	1.726	1.526	72.813	2.16
250	99.0	92.0	108.0	99.7	1.780	1.573	77.402	2.22
260	104.0	96.0	113.0	104.3	1.863	1.647	84.820	2.33
270	106.0	100.0	115.0	107.0	1.911	1.689	89.212	2.39
280	110.0	103.0	120.0	111.0	1.982	1.752	96.006	2.48
290	113.0	106.0	125.0	114.7	2.048	1.810	102.454	2.56
300	117.0	109.0	129.0	118.3	2.113	1.868	109.111	2.64
310	122.0	113.0	133.0	122.7	2.190	1.936	117.248	2.74
320	123.0	115.0	136.0	124.7	2.226	1.968	121.103	2.78
330	126.0	118.0	141.0	128.3	2.292	2.026	128.331	2.86
340	129.0	120.0	142.0	130.3	2.327	2.057	132.362	2.91

350	132.0	125.0	149.0	135.3	2.417	2.136	142.713	3.02
360	134.0	128.0	151.0	137.7	2.458	2.173	147.677	3.07
370	137.0	129.0	154.0	140.0	2.500	2.210	152.725	3.13
380	140.0	131.0	157.0	142.7	2.548	2.252	158.598	3.18
390	142.0	135.0	160.0	145.7	2.601	2.299	165.339	3.25
400	145.0	136.0	164.0	148.3	2.649	2.341	171.448	3.31
450	155.0	149.0	172.0	158.7	2.833	2.504	196.167	3.54

Table S2.

Ultrasound Olympus 500kHz transducer intensity calibration for in vitro stimulation.

	Olympus 500 kHz	0.5	<-frequency (MHz)		
mVRMS	Output (mVpp)	Negative Pressure (Mpa)	Corrected Pressure = Prms (Mpa)	Intensity (100%) (W/cm2)	Mechanical Index
100	143	0.105	0.092	0.267	0.131
120	171	0.125	0.110	0.382	0.156
140	201	0.147	0.130	0.528	0.184
160	227	0.166	0.147	0.673	0.207
180	253	0.185	0.163	0.836	0.231
200	281	0.205	0.182	1.031	0.257
220	310	0.227	0.200	1.255	0.283
240	336	0.246	0.217	1.474	0.307
260	360	0.263	0.233	1.692	0.329
280	378	0.276	0.244	1.866	0.345
300	390	0.285	0.252	1.986	0.356
320	400	0.292	0.258	2.089	0.365
340	410	0.300	0.265	2.195	0.375
360	418	0.306	0.270	2.281	0.382
380	422	0.308	0.273	2.325	0.386
400	426	0.311	0.275	2.370	0.389
420	426	0.311	0.275	2.370	0.389
440	426	0.311	0.275	2.370	0.389
460	430	0.314	0.278	2.414	0.393
480	430	0.314	0.278	2.414	0.393
500	430	0.314	0.278	2.414	0.393
520	432	0.316	0.279	2.437	0.395
540	434	0.317	0.280	2.459	0.397
560	434	0.317	0.280	2.459	0.397
580	434	0.317	0.280	2.459	0.397
600	436	0.319	0.282	2.482	0.398
620	438	0.320	0.283	2.505	0.400
640	440	0.322	0.284	2.528	0.402
660	442	0.323	0.286	2.551	0.404
680	448	0.327	0.289	2.621	0.409
700	450	0.329	0.291	2.644	0.411
720	450	0.329	0.291	2.644	0.411
740	454	0.332	0.293	2.691	0.415
760	456	0.333	0.295	2.715	0.417

780	456	0.333	0.295	2.715	0.417
800	460	0.336	0.297	2.763	0.420
820	462	0.338	0.299	2.787	0.422
840	462	0.338	0.299	2.787	0.422
860	462	0.338	0.299	2.787	0.422
880	462	0.338	0.299	2.787	0.422
900	462	0.338	0.299	2.787	0.422
920	464	0.339	0.300	2.811	0.424
940	466	0.341	0.301	2.835	0.426
960	466	0.341	0.301	2.835	0.426
980	470	0.344	0.304	2.884	0.429
1000	474	0.346	0.306	2.934	0.433

Movie S1.
Functional walking gait in normal control group.

Movie S2.
Functional walking gait in partial crush injury model (PCI) group.

Movie S3.
Functional walking gait in LI-cTBUS-treated PCI group.